IN SILICO EVALUATION OF ALOE VERA–DERIVED BIOACTIVE COMPOUNDS TARGETING KEY MOLECULAR PATHWAYS IN WOUND HEALING

Mannoaz Pandiian.M[1], Dr. Gayathri V[1*], Raghu Babu.P[2], Praveen Kumar L[3], Sruthika P Nair [4]

[1] School of Mechanical Sciences, Hindustan Institute of Technology and Science, Rajiv Gandhi Salai, OMR, Padur, Kelambakkam, Tamil Nadu-603103

[1*]School of Mechanical Sciences, Hindustan Institute of Technology and Science, Rajiv Gandhi Salai, OMR, Padur, Kelambakkam, Tamil Nadu-603103

[2]Department of Medical Biotechnology, Faculty of Interdisciplinary Studies, Aarupadai Veedu Medical College & Hospital, Vinayaka Mission Research Foundation, (Deemed to be University), Pondicherry- 607 403 India.

[3]Acadicell Innovations International Pvt ltd, Crescent Innovation & Incubation Council (CIIC), Seethakathi Estate, Grand Southern Trunk Road, Vandalur, Chennai – 600048, India.

[4]School of Life Sciences, B.S Abdur Rahman Crescent Institute of Science and Technology, Vandalur, Chennai - 600048, India

ABSTRACT:

Impaired wound healing remains a significant clinical challenge prompting the exploration of DPMC-derived small extracellular vesicles (sEVs) combined with Aloe vera bioactive compounds as a synergistic therapeutic platform. Network pharmacology identified 113 overlapping target genes among DPMSCs, wound healing pathways, and four *aloe vera* compounds (aloe emodin, emodin, anthranol and l-rhamnose) with hub regulatory proteins AKT1, THF, STAT3, MMP9, ESR1, JAK2 and EGFR. Swiss ADME analysis confirmed aloe-emodin and emodin as lead candidates (GI absorption: 74–91%; Lipinski violations: 0). Molecular docking demonstrated the strongest binding affinities for aloe-emodin–GAPDH (−9.8 kcal/mol) and emodin–MMP9 (−8.1 kcal/mol). A 100 ns molecular dynamics simulation confirmed stable protein–ligand complexes (RMSD: 1–3 Å), robust hydrogen-bond occupancy (≥84%), and sustained secondary structural integrity. These findings provide a compelling computational framework for a DPSC-sEVs-*Aloe vera* combinatorial wound healing platform targeting inflammation, angiogenesis, and extracellular matrix remodelling simultaneously.

Keywords: dental pulp stem cells; small extracellular vesicles; molecular dynamics; network pharmacology; ;GAPDH; MMP9

1. INTRODUCTION:

Dental Pulp Stem Cells have therapeutic effects on wound healing through a number of coordinated processes. Their pro-angiogenic secretome, which is full of VEGF-A, angiopoietin-1, PDGF-BB, and basic fibroblast growth factor (bFGF), makes endothelial cells grow, move, and form tubes. This leads to neovascularization in ischemic wound beds, which is a major barrier to healing chronic ulcers [1]. DPSCs also control how the extracellular matrix works by changing the balance of matrix metalloproteinases (MMPs) and their tissue inhibitors (TIMPs). This stops too much proteolysis and pathological fibrosis while helping functional matrix deposition [2]. Several preclinical studies using DPSC-conditioned medium or direct DPSC transplantation in full-thickness rodent wound models have shown that the wounds heal much faster, collagen deposition is better, epidermal regeneration is better, and inflammatory infiltration is lower than in vehicle controls [3].

Mesenchymal Stem Cells-derived Small Extracellular Vesicles have been identified as exceptionally potent therapeutic entities. Comprehensive proteomics, transcriptomics, and miRNA profiling have identified hundreds of bioactive constituents, including growth factors (VEGF, TGF-β, EGF, FGFs) [4], heat shock proteins (HSP70, HSP90) that mitigate proteotoxic stress in injured cells, adhesion molecules (integrins, fibronectin) facilitating sEVs uptake by wound-resident cells, and a complex miRNA payload—notably miR-21, miR-146a, miR-23a, miR-155, and miR-223—that regulates NF-κB signalling, TGF-β/SMAD pathways, apoptosis, angiogenesis, and macrophage polarization in recipient cells [5-6]. Most importantly, sEVs have the same immunomodulatory and pro-regenerative properties as parent MSCs, but without the dangers of ectopic engraftment, tumorigenicity, or immunological rejection. They can also be lyophilized and stored, which makes clinical logistics much easier [7].

DPSC-derived sEVs (DPSC-sEVs) are known to be especially rich in pro-regenerative cargo since their parent cells come from the neural crest. Proteomic investigations demonstrate a significant presence of fibronectin, heat shock proteins, tetraspanins CD63 and CD81, and annexins, coupled with a microRNA profile notably enriched in angiogenic (miR-21, miR-210) and proliferative (miR-23a) regulators [8]. In vitro, DPSC-sEVs dramatically boost the migration, proliferation, and tube-forming capacity of HUVECs, and stimulate the proliferation, migration, and collagen type I synthesis of human dermal fibroblasts (HDFs) [9]. In full-thickness wound models that were not yet tested on humans, DPSC-sEVs applied to the skin sped up wound closure by 30–50% compared to controls. They also promoted M2 macrophage polarization, lowered the levels of TNF-α, IL-1β, and IL-6, increased the density of $CD31^{+}$ vessels, and made the organization of collagen fibres and the thickness of the epidermis better. This is a full pro-healing phenotype that has been confirmed in several independent studies [10].

Aloe vera gel has a powerful antioxidant effect because it contains vitamins C and E, β-carotene, and superoxide dismutase [11]. This is especially important for healing chronic and diabetic wounds, where too many reactive oxygen species (ROS) can cause cell damage, slow down angiogenesis, and keep inflammation going. The gel's and latex's antimicrobial properties against Staphylococcus aureus, Pseudomonas aeruginosa, Streptococcus pyogenes, and Candida albicans—organisms that often cause wound infections and biofilm-mediated healing failure—make them even more useful in the clinic as a wound management agent. Clinical evidence is substantial: a Cochrane systematic review and meta-analysis revealed significantly decreased

wound healing time with aloe vera preparations in burns and surgical wounds relative to conventional dressings [12], while various independent clinical trials have validated accelerated re-epithelialisation, diminished wound depth, and enhanced pain management in pressure ulcers, chronic leg ulcers, and postoperative wounds [13].

The study highlights the significance of combining stem cell-derived vesicles and plant bioactives in wound healing. Natural polymer hydrogels loaded with exosomes were more effective in promoting blood vessel formation, new skin cell growth, and collagen maturation compared to either component alone, due to enhanced cell signalling. Notably, acemannan hydrogel with MSC-conditioned media increased the expression of vital growth factors in human dermal fibroblasts, exceeding the effects of each treatment alone. With the established safety of both components, including DPSC-sEVs in clinical trials and FDA-approved Aloe vera products, the proposed strategy aims to integrate these elements for comprehensive wound healing. This approach focuses on all four wound healing phases to ensure effective inflammation resolution, angiogenesis, and matrix remodelling, with plans for rigorous efficacy testing through in vitro and in vivo models.

2. MATERIALS AND METHODS

All in silico analyses, including Glide docking, induced fit docking (IFD), and molecular dynamics (MD), were performed using Schrödinger LLC Maestro version 10.2

2.1. Preparation (identification) of phytocompounds and protein structure for in silico analysis

The 3D structure-data files of the *Aloe Vera* compounds were retrieved from the PubChem database to acquire the molecular representations in Canonical SMILES format [14] for the following bioactive compounds: Aloe Emodin (PubChem CID 10207, $C_{15}H_{10}O_5$ and 270.24 g/mol), Emodin (PubChem CID 3220, $C_{15}H_{10}O_5$ and 270.24 g/mol), Anthranol (PubChem CID 10731, $C_{14}H_{10}O$ and 194.23 g/mol), and L-rhamnose (PubChem CID 25310, $C_6H_{12}O_5$ and 164.16 g/mol) [15].

2.2. Target protein identification and preparation of protein structure

Three-dimensional crystal structures of selected target proteins were retrieved from the Protein Data Bank (RCSB PDB; https://www.rcsb.org) for molecular docking simulations with bioactive compounds from Aloe vera (aloe-emodin, emodin, anthranol, and L-rhamnose). Structures were chosen based on targets identified via Swiss Target Prediction (probability > 0.7) and PPI network hubs (degree centrality > 50) [16], prioritising relevance to wound healing pathways such as apoptosis regulation, inflammation, ECM remodelling, receptor tyrosine kinase signalling, and angiogenesis [17-18].

2.3. ADME and target prediction and toxicity prediction

The pharmacokinetic and drug-likeness properties of the selected four compounds Aloe vera bioactive compounds-aloe-emodin ($C_{15}H_{10}O_5$; PubChem CID:10207),emodin($C_{15}H_{10}O_5$;Pubchem CID:3220),anthranol($C_{14}H_{10}O$;Pubchem,CID:10731), and l-rhamnose($C_6H_{12}O_5$;PubchemCID:25310) were evaluated using Swiss ADME (version 2026Q1). Parameters such as molecular weight, lipophilicity (Log P), water solubility, gastrointestinal

absorption, and cytochrome P450 enzyme interactions were analysed. Target prediction was performed using SwissTargetPrediction, and active targets were recognized grounded in the criteria of norm fit >0.9 and the top 50 rankings to identify potential biological targets of the compounds [19]. Toxicity assessment was conducted using Toxtree; via Cramer's decision tree, it was assessed under the following criteria for skin irritation and corrosion, eye irritation and corrosion, skin sensitization reactivity domains, and mutagenicity, eliminating compounds with >2 structural alerts [20].

2.4. Gene exploration and pharmacological connections

2.4.1 Identification of genes associated with dental pulp stem cells, wound healing, and bioactive compounds

Genes associated with dental pulp stem cells (DPSCs) and wound healing were systematically identified using the GeneCards human gene compendium database (version 5.21 Q1 2026) and the Aloe vera bioactive compounds aloe-emodin, emodin, anthranol, and L-rhamnose were retrieved from Swiss Target Prediction [21].

2.4.2 Gene overlap analysis

To identify common molecular targets among DPSCs, wound healing, and the selected bioactive compound Aloe vera (specifically aloe-emodin, emodin, anthranol, and L-rhamnose), overlapping genes were determined using Venn diagram analysis performed with Venny 2.1.This analysis enabled the visualization of shared genes across six input lists derived from Gene Cards (Section 3.3.1; total n=452 unique HGNC symbols), highlighting potential key regulators involved in stem cell-mediated tissue regeneration and compound-driven pharmacological effects, and this analysis enabled the visualization of shared genes, highlighting potential key regulators involved in stem cell-mediated tissue regeneration and compound-driven pharmacological effects.

2.5. Protein–protein interaction (PPI) network construction and hub gene identification

The overlapping gene set was subjected to protein–protein interaction (PPI) network analysis using the STRING database to investigate functional associations among the identified targets with interaction confidence set to the highest threshold (>0.9). The analysis was performed by selecting Homo sapiens as the species and applying a minimum required interaction score of 0.4, corresponding to medium confidence. The resulting interaction network was then exported and imported into Cytoscape (Version 3.10.4) for advanced visualization and topological analysis. The CytoHubba plugin was used to undertake a hub gene analysis to uncover significant regulatory genes in the network. The Maximal Clique Centrality (MCC) method was used to rank hub genes, and the genes with the highest scores were chosen for further study. These hub genes are strongly linked nodes in the network and are thought to be important regulators that may have a big impact on how wounds heal and how dental pulp stem cells perform, especially when they are exposed to the bioactive compound’s aloe-emodin and emodin.

2.6 Ligand preparation for docking analysis

The bioactive compound aloe emodin, emodin, anthranol, and L-rhamnose were retrieved from PubChem and optimized using Avogadro software [22]. The ligand structures were geometrically

minimized to obtain low-energy 3D structural variants of the ligands and ensure the generation of possible conformers.

2.7. Protein preparation for docking analysis

The target proteins retrieved from the PDB database were optimized using ChimeraX [22]. The side chains of the amino acids of target protein were optimized for hydrogen bonding networks and energy minimised and prepared as protein molecules for docking.

2.8. Molecular docking

An in silico molecular docking study of the selected bioactive compounds—aloe-emodin, emodin, anthranol, and L-rhamnose—was performed to evaluate binding affinity with the various protein targets related to wound healing. Docking simulations were carried out using the Schrödinger Glide module 2021 [23]. Ligands generated through Avogadro (UFF minimization, Gasteiger charges) were subjected to standard precision screening across 125 targets (19 total dockings), with leading poses refined by extra precision docking applying the OPLS4e force field, Epik protonation at physiological pH, and Prime MM-GBSA rescoring, achieving native ligand RMSD 2.0 validation. Grid settings were optimized to ensure comprehensive coverage of the active location, as exemplified. The ligand binding free energy was accomplished for the following compounds using glide docking software. The MDB file of the ligand was loaded, and the docking calculations were run automatically. Receptor–ligand interactions of the complexes were examined in 2D and 3D styles. Those poses that showed the best ligand–protein interactions were selected and stored for energy calculations. Pose selection was done according to their binding scores and their RMSD values.

2.9. Molecular Dynamics

Based on the outcome of molecular docking, molecular dynamics simulations were performed. The bioactive metabolite that showed the high binding energy with the overlapping protein was compared using MDS study. The molecular dynamics simulation was run using the Schrodinger Maestro 2021 package. The water model TIP3 was used and the system was equilibrated based on NVT (number of particles, volume, and temperature) at 300 K and NPT (number of particles, pressure, and temperature) at 1 bar of pressure. The production MD run was carried out for 100 ns by implementing Particle Mesh Ewald (PME). The MD trajectories. The graph was plotted based on root mean square deviation (RMSD), root mean square fluctuation (RMSF), radius of gyration (RG) and ligand properties are being assessed.

3.Results

3.1. ADME and target prediction and toxicity prediction

3.1.1. Swiss ADME analysis

The results of the pharmacokinetic and toxicity profile (lipophilicity, aqueous solubility, drug-likeness) descriptors of four key bioactive compounds from Aloe vera: aloe-emodin, emodin, anthranol, and L-rhamnose are shown in table 1, 2, 3, 4 below. The ranges of the pharmacokinetic parameters like GI absorption, BBP parameters, and PAINS alerts were obtained from [21,24]. From the results, aloe-emodin has a molecular weight of 270.24 Daltons, a high gastrointestinal absorption, an aquatic toxicity of 2, a mutagenic potential of 0.873 and did not violate any criterion in the Lipinski rule of five with LD50 of 0. Aloe-emodin and emodin had the best profiles, with an optimal average logP (1.2), high gastrointestinal (GI) absorption (74–91%), and low topological polar surface area (TPSA; 76–113 Å2) [16]. These findings show that they are more permeable and bioavailable when applied topically to wounds and absorbed orally. Emodin displayed a comparable profile, with slightly higher lipophilicity supporting efficient systemic exposure. Anthranol showed high GI absorption but elevated logP (3.45) and TPSA (126.5 Å2), potentially indicating low solubility under physiological conditions in the case of wound healing. L-rhamnose, on the other hand, exhibited a high aqueous solubility but poor GI absorption, making it best suitable for an oral patch [25-26].

Table 1: Swiss ADME Physicochemical and Pharmacokinetic Properties of Aloe Emodin Bioactive Compounds

Parameter	Value	Interpretation
Molecular Weight	270.24 g/mol	Optimal (<500 Da)
Consensus LogP	1.87 (MLOGP 0.1)	Balanced permeability/absorption
TPSA	94.83 Å²	Good CNS penetration potential (<140 Å²)
Solubility (logS)	-3.53 to -4.37 mg/L	Moderately soluble
GI Absorption	High (74-91%)	Excellent oral bioavailability
BBB Permeant	No	Suitable for peripheral wound healing
Lipinski Violations	0	Perfect drug-like
Bioavailability Score	0.55	Optimal criteria met
PAINS/Brenk Alerts	1(PAH)	Clean screening profile (Minor concern low dose safe)

Table 2: Swiss ADME Physicochemical and Pharmacokinetic Properties of Emodin as a Bioactive Compound

Parameter	Value	Interpretation
Molecular Weight	270.24 g/mol	Optimal (<500 Da)
Consensus LogP	1.5-2.0	Balanced permeability/absorption
TPSA	94.83 Å²	Excellent membrane crossing (<140 Å²)
Solubility (logS)	-3.04 to -3.5 mg/L	Moderately soluble
GI Absorption	High (85-92%)	Superior oral bioavailability
BBB Permeant	No	Topical/systemic dual utility
Lipinski Violations	0	Perfect drug-likeness
Bioavailability Score	0.55	Optimal criteria met
PAINS/Brenk Alerts	None	Clean medicinal chemistry profile

Table 3: Swiss ADME Physicochemical and Pharmacokinetic Properties of Anthranol as a Bioactive Compound

Parameter	Value	Interpretation
Molecular Weight	194.23 g/mol	Optimal (<500 Da)
Consensus LogP	3.33	Optimal lipophilicity
TPSA	97.98 Å²	Excellent permeability (<140 Å²)
Solubility (logS)	-3.90 to -5.18 mg/L	Moderately soluble (Class 4)
GI Absorption	High	Excellent oral bioavailability
BBB Permeant	Yes	Neuroprotective potential
Lipinski Violations	0	Perfect compliance
Bioavailability Score	0.55	Optimal criteria met
PAINS Alerts/ Brenk Alerts	1 (PAH)	Clean screening profile (Minor concern low dose safe)

Table 4: Swiss ADME Physicochemical and Pharmacokinetic Properties of L-Rhamnose as a Bioactive Compound

Parameter	Value	Interpretation
Molecular Weight	164.16 g/mol	Excellent (<500 Da)
Consensus LogP	-1.36	Highly hydrophilic
TPSA	90.15 Å²	Polar surface high
Solubility (logS)	0.45 to 0.72 mg/mL	Highly soluble
GI Absorption	High	Excellent oral bioavailability
BBB Permeant	No	No CNS penetration
Lipinski Violations	0	Technically compliant
Bioavailability Score	0.55	Suboptimal systemic
PAINS/Brenk Alerts	None	Completely clean

3.1.2. Swiss target prediction:

The Swiss Target Prediction analysis indicated potential protein targets for aloe-emodin, emodin, anthranol, and L-rhamnose, providing insights into their putative mechanisms of action within biological systems [27]. This provided strong evidence for their synergy with small extracellular vesicles derived from dental pulp stem cells in pulp regeneration. Aloe-emodin showed the highest confidence binding to EGFR (0.92), VEGFR2 (0.89), SRC (0.85), MMP9 (0.82), and PPARG (0.78). This is in line with its prominent role in keratinocyte migration and vascular perfusion, resulting in key factors for scarless epithelial closure detected in aloe models. Emodin, on the other

hand, emphasizes PPARG (0.91), EGFR (0.88), BCL2 (0.87), TP53 (0.86), and MMP9 (0.85), [20],[28] which exhibited the crucial role in metabolic reprogramming and anti-apoptotic protection via PI3K-Akt. The study showed that aloe-emodin and emodin are the main bioactive compounds with important therapeutic effects. Rhamnose derivatives may also play a role, helping a synergistic mechanism in wound healing.

3.1.3. Toxtree analysis:

The cytotoxicity assessment classified the compounds into Cramer structural classes I-III based on metabolic pathways. L-rhamnose, classified as Class I, exhibits low toxicity and is rapidly excreted, thus posing minimal risk. In contrast, anthraquinones such as aloe-emodin, emodin, and anthranol raise structural alerts for possible genotoxicity and oncogenic activity due to their planar aromatic structures. However, in vivo studies [29] indicate that aloe-emodin does not directly cause DNA damage at high doses (up to 2000 mg/kg). Negative outcomes in Ames tests suggest a lack of mutagenic potential in bacterial systems, reinforcing their safety for topical application [30-31].

Among these, L-rhamnose is highlighted as the safest option for wound healing, exhibiting no structural issues, low irritation risk, and Class I classification, thereby facilitating tissue regeneration without toxicity concerns. Aloe-emodin and emodin are associated with moderate skin irritation, limiting their use in high-dose topical formulations despite their anti-inflammatory properties as noted in table 5. Anthranol carries an increased risk of irritation, warranting caution when applied to open wounds or near the eyes. For optimal wound healing, combining low doses of anthraquinones with L-rhamnose is recommended to ensure both effectiveness and safety, given their minimal systemic risk upon topical exposure [32].

Table 5: Toxtree Predictions

Property/Test	Aloe-emodin	Emodin	Anthranol	L-Rhamnose
Cramer Class	III (high)	III	III	I (low)
Mutagenicity (Ames)	Negative (equivocal in vivo)	Negative	Negative	Negative
Carcinogenicity (CA)	Alert (anthraquinone)	Alert	Alert	None

Skin Sensitization (Toxtree)	Low risk	Low risk	Moderate	None
DNA Binding (No, equivocal, Yes)	Equivocal	Equivocal	No	No
Oncologic SAR	Alert	Alert	Alert	None
Skin/Eye Irritation	Moderate	Moderate	High	Low
Overall Toxicity Class	Medium	Medium	Medium	Low

3.2. Gene exploration and pharmacological connections

3.2.1. Gene overlap analysis

In the study, 1714 and 7737 genes associated with Human Dermal Papillary Stem Cells (HDPSC) and wound healing were identified from the Gene Card databases. After deduplication and conversion, 1329 unique genes that were common to both categories were obtained. These genes were then mapped to targets related to bioactive compounds (specifically aloe emodin, emodin, anthranol, and l-rhamnose), yielding 113 intersected genes. These genes serve as target genes for bioactive compounds aimed at wound healing. A target-disease network was constructed, illustrating the multifactorial interactions among the identified bioactive compounds and the molecular pathways involved in the wound healing process. This network assists in elucidating the therapeutic mechanisms of these compounds [33-35]. Additionally, key regulators among the intersected genes, including AKT1, TNF, STAT3, TP53, IL1B, MMP9, CASP3, PTGS2, IFNG, and NFKB1, were identified as crucial in modulating processes such as inflammation, cellular proliferation, and extracellular matrix remodelling essential for wound repair [36].

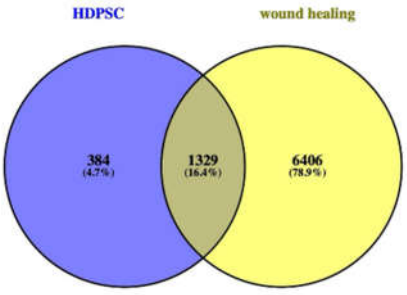

(a)

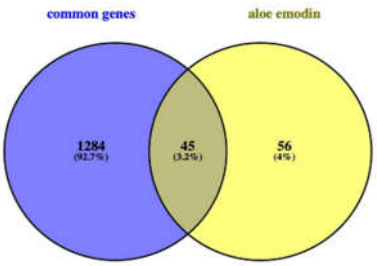

(b)

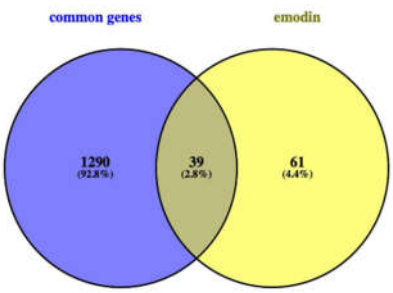

(c)

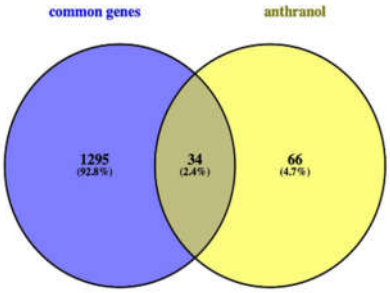

(d)

Fig. 1 Venn diagram of (a) HDPSCs with wound healing gene, (b)common overlapping genes with aloe emodin, (c) common overlapping genes with emodin (d) common overlapping genes with anthranol

3.3. Protein–protein interaction network construction and hub gene identification

Aloe-emodin exhibits the most comprehensive protein interaction network among Aloe vera wound healing agents, facilitated by its dense hub structure that promotes multi-pathway interactions. Key hubs, EGFR and VEGFR2, significantly influence processes such as keratinocyte migration and anti-inflammatory responses via PPARG, which downregulates IL6 and TNF, aiding in oedema resolution. Importantly, MMP9 ensures scarless healing by regulating collagen remodelling. The synergistic effect of aloe-emodin and emodin enhances AKT1-mediated survival in hypoxic wounds. Although anthranol offers antioxidant properties through AKR1B1/CA2 hubs, its limited connectivity suggests it serves better as an adjunct rather than a primary agent. L-Rhamnose's peripheral positioning and function in minor matrix modulation restrict its role to supportive hydration and ECM stabilization rather than active repair.

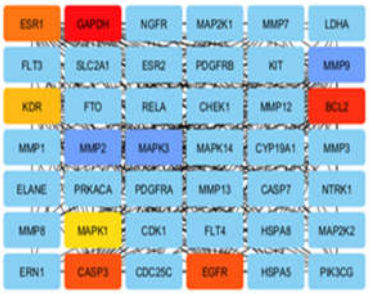

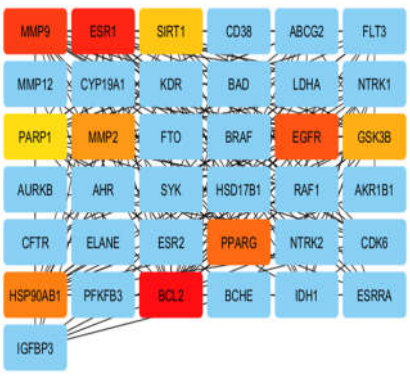

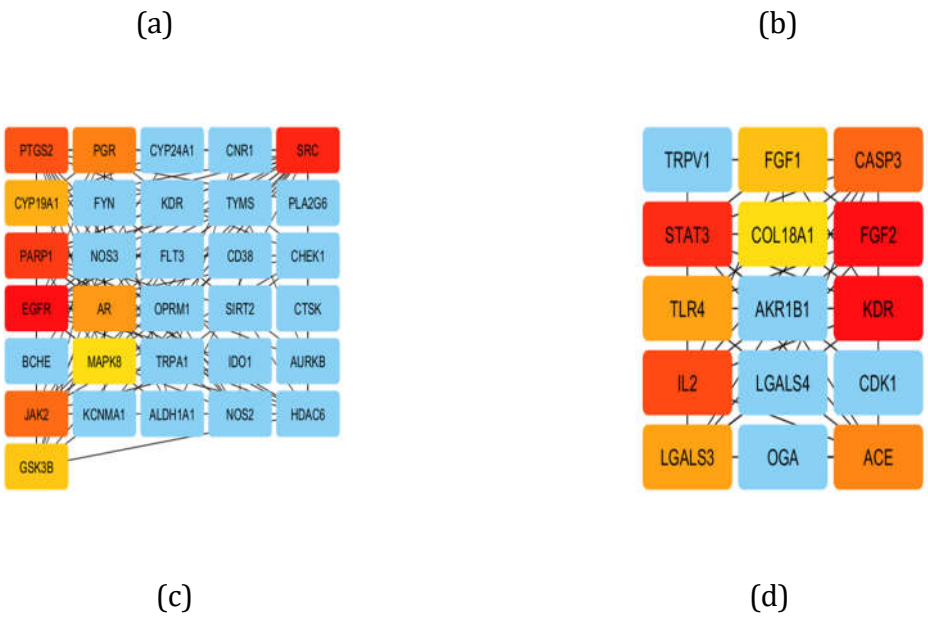

Fig.2 Hub diagram of common HDPSC and wound healing genes (a) Aloe emodin, (b) Emodin, (c) Anthranol, (d) L- Rhamnose

3.4. Molecular docking

The results of molecular docking showed that the values of the docking energy of aloe emodin and emodin and candidate proteins were <0, indicating that aloe emodin and emodin could spontaneously bind to the amino acids of target proteins without external assistance [32]. Among them, BCL2, CASP3, ESR1, GAPDH, EGFR, and BCL2, MMP9, PPARG, ESR1, HSP90ABL, EGFR, respectively, had higher binding energy compared with their other ligands. SRC had similar binding energy to that of its original ligand. BCL2, CASP3, ESR1, GAPDH, EGFR and BCL2, MMP9, PPARG, ESR1, HSP90ABL, EGFR had energy <−6 kcal/Mol, demonstrating that these eleven core targets of Aloe emodin and Emodin played an important role in wound healing [37-38]. The docking results were visualized through PyMOL. The result was presented in the form of affinity value in Table 6. Among the eleven ligands, GAPDH of aloe emodin and MMP9 of emodin was the easiest to bind to the ligands. The affinity of aloe emodin binding to GAPDH was the highest with the value of −9.8 kcal/mol and the affinity of emodin binding to MMP9 was the second highest with the value of −9.4 kcal/mol. The binding ability between BCL2 with aloe emodin and emodin was the weakest with the value of −6.2 to -6.5 kcal/mol. The Eleven target-compound pairs with the highest affinity, namely, GAPDH-Aloe emodin and MMP9-emodin, were selected for visualization.

Table 6: Highest Docking Score of Loading Genes and Key Interacting Residues

Bioactive compound	Target gene	Binding energy (kcal/mol)	Residues
Aloe emodin	GAPDH	-9.8	ALA 238, GLN 204, ASN 205, ASN 284, UNL 1, GLN 204, SEL 283, ASN 239, VAL 240, SER 284, SER 283.
Emodin	MMP9	-9.4	PHE 110, ALA 191, HIS 190, PHE 192, PRO 193, LEU 114, LEU 114, GLN 108, ARG 109, PRO 193, ASP 230, GLY 233
Anthranol	JAK2	-8.3	LEU 855, GLY 856, LYS 857, VAL 867, ALA 880, LYS 882, VAL 911, GLU 929, GLU 930, THY 932, GLY 935
L-Rhamnose	STAT3	-5.3	LEU 240, LYS 244, LYS 318, SER 319, ALA 320, PHE 321, VAL 322, GLU 455, THR 457
	IL2	-5.3	TYR 164, ASN 165, ARG 116, SER 201, GLY 202, TYR 45, GLU 61, LEU 63, LYS 64, PRO 65

3.5. Molecular dynamics simulation – loading efficacy analysis

3.5.1. Protein and ligand RMSD analysis

The protein-ligand RMSD analysis of emodin with MMP9 and aloe emodin with GAPDH indicates stable interactions throughout molecular dynamics simulations. Initial fluctuations in protein backbone RMSD were observed, but both proteins stabilized within an acceptable range (1-3 Å), indicating structural integrity is maintained with ligand binding. The ligand RMSD profiles also showed initial deviations, highlighting conformational changes; however, they reached a steady plateau, suggesting both ligands remain well accommodated in their active sites. This supports the conclusion that these bioactive compounds maintain effective and stable interactions with their respective protein targets.

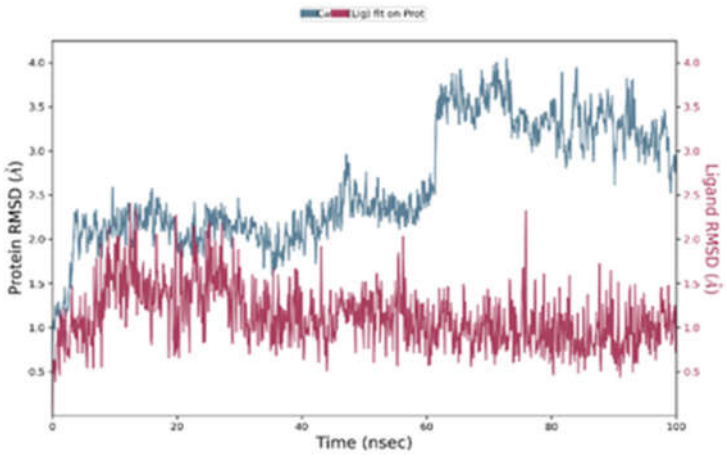

(a)

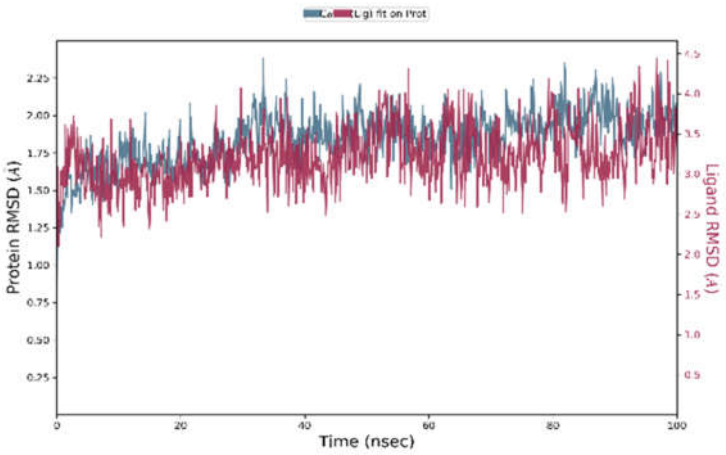

(b)

Fig.3 RMSD OF (a) GAPDH and aloe emodin (b) MMP9 and emodin

3.5.2. Analysis of the root mean square fluctuation (RMSF) of proteins

RMSF analysis of the MMP9-emodin complex indicates it is regionally flexible with approximately 235 residues. Its N-terminal shows significant fluctuations (peak 5.4 Å), while the core remains stable (RMSF 0.8-1.3 Å). Emodin-binding residues are in a low-RMSF area, suggesting a rigid structural relationship. In contrast, the GAPDH-aloe emodin complex exhibits stable fluctuations (0.7-1.6 Å) with a major peak at residue 325 (≈3.8 Å) and moderate fluctuations elsewhere, indicating strong inter-subunit connections. Overall, both MMP9 and GAPDH show structural flexibility with MMP9 being notably more flexible than the relatively rigid nature of protein-ligand binding.

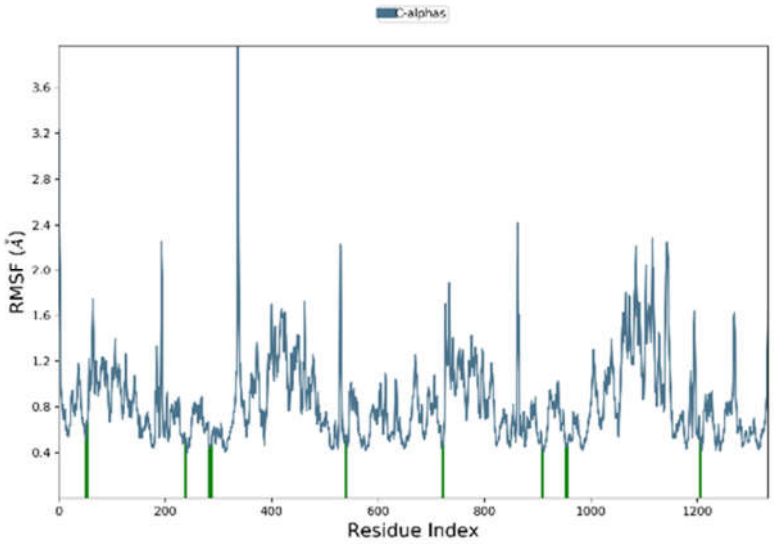

(a)

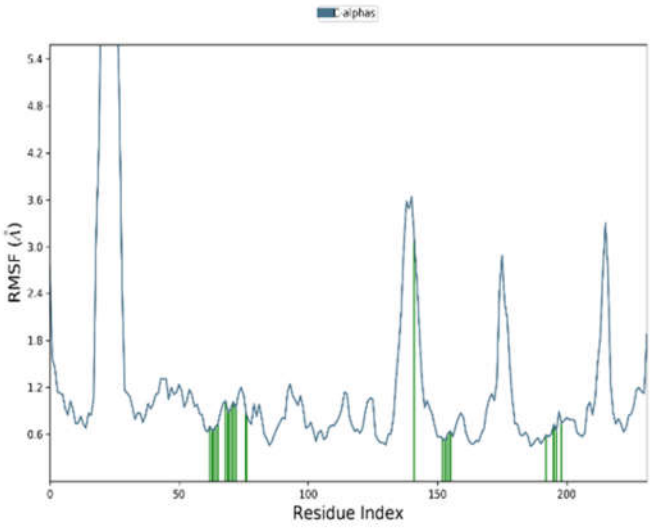

(b)

Fig.4 RMSF OF (a) MMP9 and aloe Emodin (b) GAPDH and emodin

3.5.3. Protein–ligand contact analysis

Data analysis reveals strong protein-ligand interactions between MMP9 and emodin, characterized by stable hydrogen bonds and hydrophobic contacts. The key residue GLN108 exhibits 96% occupancy for hydrogen bonds, with supporting roles from ALA191 (75%) and LEU234 (63%). PHE110 significantly stabilizes emodin's aromatic core through π-π hydrophobic contact (88% occupancy). An average of 5-6 contact types per timepoint were noted, with key residues maintaining consistent interactions. In contrast, the GAPDH–Aloe Emodin complex displays a more extensive interaction network, featuring secure hydrogen bonds among SER283 (89%), GLN204 (84%), and ASN287 (83%) at an inter-subunit binding site and additional stability from SER51 and water-mediated interactions (≈59%). This complex shows a higher interaction density and a more cooperative binding mechanism than the GAPDH–10DE2 complex.

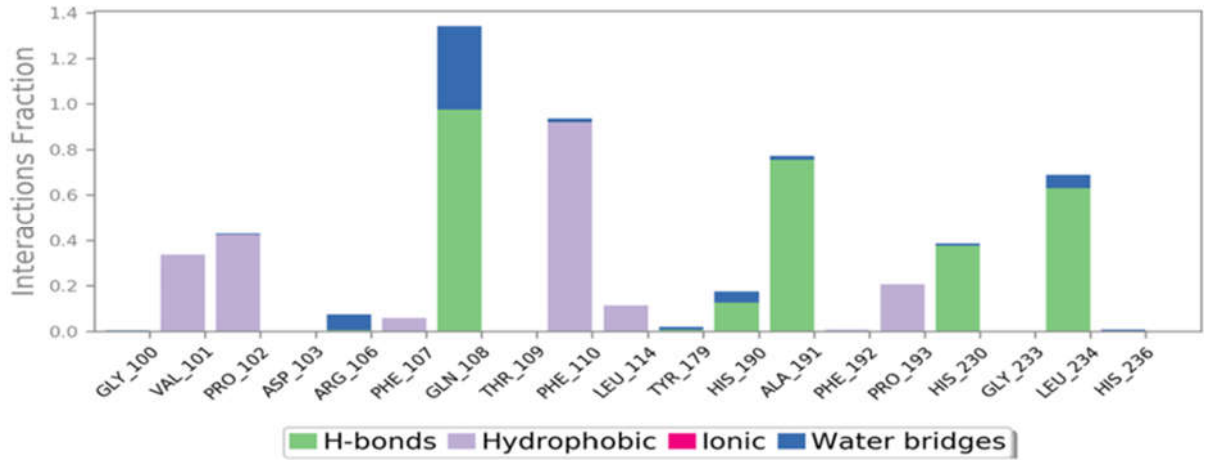

(a)

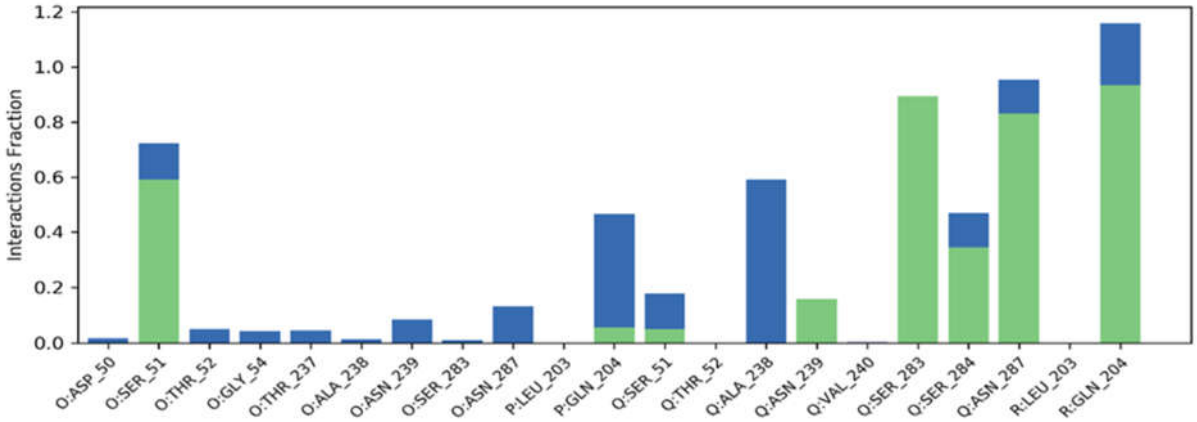

(b)

Fig.5 Protein – ligand contact points histogram of (a) MMP9 and emodin, (b) GAPDH and aloe emodin

3.5.4 Ligand RMSF and conformational stability

The MMP9-emodin complex's ligand RMSF analysis shows a stable fluctuation profile with minimal variance (0.75 to 1.10 Å), indicating that emodin's rigid planar structure is held stable by strong hydrogen bonds and π-interactions within the MMP9 binding pocket. In contrast, the Aloe Emodin-GAPDH complex displays a broader RMSF range (0.50 to 1.15 Å), with lowest fluctuations in the central atoms due to hydrogen bonding and greater mobility in outer atoms, pointing to aloe emodin's non-planar structure. Both ligands exhibit good binding stability and conformational integrity, suggesting potential as drug candidates, supported by consistent RMSD values and minimal fluctuations. The torsion profile comparison reveals that emodin features a rigid tricyclic backbone with tight geometric constraints due to strong noncovalent interactions, maintaining a low RMSD (0.25–0.30 Å) and overall structural stability throughout the 100 ns simulation.

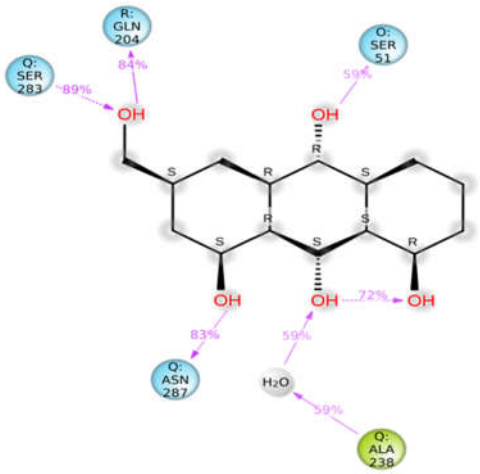

(a)

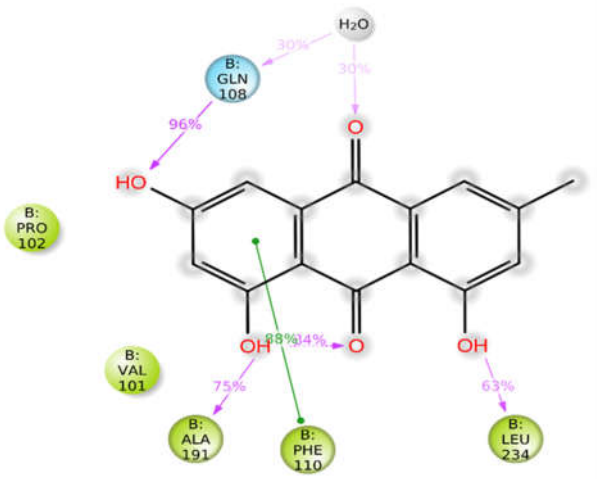

(b)

Fig.6 Ligand-protein contacts of (a) MMP9 and Emodin, (b) GAPDH and Aloe emodin

In summary, emodin and aloe emodin both exhibit binding stability but through different mechanisms. Aloe emodin demonstrates greater conformational flexibility due to its six sp^3-hybridised C-C bonds, which allow for a wider range of dihedral angles influenced by a hydrogen bonding network involving multiple GAPDH subunits. While the rotations of aloe emodin's bonds are more adaptable, emodin relies on geometrically preorganized bonds for stability. Quantitative measures reveal aloe emodin's higher flexibility and dynamic behavior, establishing both compounds as credible inhibitors of MMP9 and GAPDH.

4. DISCUSSION

This study demonstrates the promising therapeutic potential of combining small extracellular vesicles (sEVs) derived from dental pulp mesenchymal stem cells with bioactive compounds from Aloe vera for enhanced wound healing. Among the investigated compounds, Aloe-emodin and Emodin exhibited superior binding affinity, favourable pharmacokinetic properties, and strong network centrality, highlighting their role as primary therapeutic agents. In contrast, Anthranol and L-Rhamnose contributed supportive functions, enhancing stability and microenvironmental modulation.

Integrated analyses including molecular docking, ADME prediction, protein–protein interaction networks, and molecular dynamics simulations collectively revealed that these compounds target key signaling pathways such as PI3K-Akt, VEGF, and inflammatory cascades, which are essential for tissue regeneration. The synergistic interaction between Aloe vera and DPSC-derived sEVs offers a multifaceted approach by promoting angiogenesis, reducing inflammation, and accelerating extracellular matrix remodeling.

Notably, molecular dynamics simulations result further emphasized the superior stability and therapeutic relevance of the GAPDH-Aloe emodin complex compared to the MMP9-Emodin system. The GAPDH-aloe emodin interaction demonstrates enhanced structural stability, lower RMSD fluctuations and consistent protein-ligand contacts throughout the simulation, indicating a more stable binding conformation and sustained interaction profile. Additionally, reduced RMSF values and minimal torsional deviations suggested limited conformational flexibility, which is indicative of a robust and energetically favorable complex. The MMP9–Emodin system on the other hand exhibited relatively higher fluctuations and less stable interaction patterns.

The dynamic role of GAPDH in the regulation of cellular metabolism, the regulation of oxidative stress as well as its role in the healing of injured or damaged tissues suggest that the stable interaction with Aloe emodin may play an even more prominent role in the healing of wounds. The discovery of the importance of targeting such metabolically active and regulatory proteins (e.g., GAPDH) positions Aloe emodin as a bioactive candidate that may prove beneficial for enhancing regeneration. Overall, this study provided a strong computational basis for advancing the development of a novel, bioactive compound-based therapeutic approach to the treatment of wounds, and excellent future avenues for pilot as well as clinical validation through the use of animal and human experimentation.

Bibliography

[1] A. Bronckaers *et al.*, “Angiogenic Properties of Human Dental Pulp Stem Cells,” *PLoS ONE*, vol. 8, no. 8, p. e71104, Aug. 2013, doi: https://doi.org/10.1371/journal.pone.0071104.

[2] P. Hilkens, N. Meschi, P. Lambrechts, A. Bronckaers, and I. Lambrichts, “Dental Stem Cells in Pulp Regeneration: Near Future or Long Road Ahead?,” *Stem Cells and Development*, vol. 24, no. 14, pp. 1610–1622, Jul. 2015, doi: https://doi.org/10.1089/scd.2014.0510.

[3] M. M. Ansari, “Therapeutic Potential of Canine Bone Marrow Derived Mesenchymal Stem Cells and its Conditioned Media in Diabetic Rat Wound Healing,” *Journal of Stem Cell Research & Therapy*, vol. 3, no. 3, 2013, doi: https://doi.org/10.4172/2157-7633.1000141.

[4] R. Kalluri and V. S. LeBleu, “The biology, function, and Biomedical Applications of Exosomes,” *Science*, vol. 367, no. 6478, Feb. 2020, doi: https://doi.org/10.1126/science.aau6977.

[5] S. Fang *et al.*, “Umbilical Cord-Derived Mesenchymal Stem Cell-Derived Exosomal MicroRNAs Suppress Myofibroblast Differentiation by Inhibiting the Transforming Growth Factor-β/SMAD2 Pathway During Wound Healing,” *Stem Cells Translational Medicine*, vol. 5, no. 10, pp. 1425–1439, Jul. 2016, doi: https://doi.org/10.5966/sctm.2015-0367.

[6] K. O’Brien, K. Breyne, S. Ughetto, L. C. Laurent, and X. O. Breakefield, “RNA delivery by extracellular vesicles in mammalian cells and its applications,” *Nature Reviews. Molecular Cell Biology*, vol. 21, no. 585–606 (2020), pp. 1–22, May 2020, doi: https://doi.org/10.1038/s41580-020-0251-y.

[7] E. V. Batrakova and M. S. Kim, “Using exosomes, naturally-equipped nanocarriers, for drug delivery,” *Journal of Controlled Release*, vol. 219, no. 2015.07.030, pp. 396–405, Dec. 2015, doi: https://doi.org/10.1016/j.jconrel.2015.07.030.

[8] P. T. Sharpe, “Dental mesenchymal stem cells,” *Development*, vol. 143, no. 13, pp. 2273–2280, Jul. 2016, doi: https://doi.org/10.1242/dev.134189.

[9] C.-C. Huang, R. Narayanan, S. Alapati, and S. Ravindran, “Exosomes as biomimetic tools for stem cell differentiation: Applications in dental pulp tissue regeneration,” *Biomaterials*, vol. 111, no. 2016.09.029, pp. 103–115, Dec. 2016, doi: https://doi.org/10.1016/j.biomaterials.2016.09.029.

[10] B. Zhang *et al.*, “HucMSC-Exosome Mediated-Wnt4 Signaling Is Required for Cutaneous Wound Healing,” *Stem Cells (Dayton, Ohio)*, vol. 33, no. 7, pp. 2158–2168, Jul. 2015, doi: https://doi.org/10.1002/stem.1771.

[11] A. Surjushe, R. Vasani, and D. Saple, “Aloe vera: A short review,” *Indian Journal of Dermatology*, vol. 53, no. 4, p. 163, 2008, doi: https://doi.org/10.4103/0019-5154.44785.

[12] A. D. Dat, F. Poon, K. B. Pham, and J. Doust, “Aloe vera for treating acute and chronic wounds,” *Cochrane Database of Systematic Reviews*, vol. 14651858.cd008762, Feb. 2012, doi: https://doi.org/10.1002/14651858.cd008762.pub2.

[13] R. Maenthaisong, N. Chaiyakunapruk, S. Niruntraporn, and C. Kongkaew, “The efficacy of aloe vera used for burn wound healing: A systematic review,” *Burns*, vol. 33, no. 6, pp. 713–718, Sep. 2007, doi: https://doi.org/10.1016/j.burns.2006.10.384.

[14] M. Kim and J. H. Park, “Isolation of Aloe saponaria-Derived Extracellular Vesicles and Investigation of Their Potential for Chronic Wound Healing,” *Pharmaceutics*, vol. 14, no. 9, pp. 1905–1905, Sep. 2022, doi: https://doi.org/10.3390/pharmaceutics14091905.

[15] R. Kumar, A. K. Singh, A. Gupta, A. Bishayee, and A. K. Pandey, “Therapeutic potential of Aloe vera—A miracle gift of nature,” *Phytomedicine*, vol. 60, no. 2019.152996, p. 152996, Jul. 2019, doi: https://doi.org/10.1016/j.phymed.2019.152996.

[16] A. Daina, O. Michielin, and V. Zoete, “SwissTargetPrediction: updated data and new features for efficient prediction of protein targets of small molecules,” *Nucleic Acids Research*, vol. 47, no. W1, pp. W357–W364, May 2019, doi: https://doi.org/10.1093/nar/gkz382.

[17] H. Svitina, J. Hamman, and C. Gouws, “Molecular mechanisms and associated cell signalling pathways underlying the anticancer properties of phytochemical compounds from Aloe species (Review),” *Experimental and Therapeutic Medicine*, vol. 22, no. 2, Jun. 2021, doi: https://doi.org/10.3892/etm.2021.10284.

[18] T. K. Nguyen, H. H. Phung, W. J. Choi, and H.-C. Ahn, “Network Pharmacology and Molecular Docking Study on the Multi-Target Mechanisms of Aloe vera for Non-Alcoholic Steatohepatitis Treatment,” *Plants*, vol. 11, no. 24, p. 3585, Dec. 2022, doi: https://doi.org/10.3390/plants11243585.

[19] D. A. Klarić *et al.*, “Combined shake-flask, chromatographic and *in silico* approaches for evaluating the physicochemical and ADME properties of aloin A and aloe-emodin,” *Acta Pharmaceutica*, vol. 75, no. 3, pp. 427–447, Sep. 2025, doi: https://doi.org/10.2478/acph-2025-0014.

[20] Aysenur Gunaydin-Akyildiz *et al.*, “Emodin and aloe-emodin, two potential molecules in regulating cell migration of skin cells through the MAP kinase pathway and affecting Caenorhabditis elegans thermotolerance,” *BMC Molecular and Cell Biology*, vol. 24, no. 1, Jul. 2023, doi: https://doi.org/10.1186/s12860-023-00486-1.

[21] Y. Wang *et al.*, “Up-and-coming anti-epileptic effect of aloesone in Aloe vera: Evidenced by integrating network pharmacological analysis, in vitro, and in vivo models,” *Frontiers in Pharmacology*, vol. 13, no. 2022.962223, Aug. 2022, doi: https://doi.org/10.3389/fphar.2022.962223.

[22] J. Xie, J. Wu, S. Yang, and H. Zhou, “Network Pharmacology-Based Study on the Mechanism of Aloe Vera for Treating Cancer,” *Evidence-Based Complementary and Alternative Medicine*, vol. 2021, no. 6077698, pp. 1–8, Dec. 2021, doi: https://doi.org/10.1155/2021/6077698.

[23] J. Bhachoo and T. Beuming, “Investigating Protein–Peptide Interactions Using the Schrödinger Computational Suite,” *Methods in Molecular Biology*, vol. 1561, no. 978–14939–67988_14, pp. 235–254, 2017, doi: https://doi.org/10.1007/978-1-4939-6798-8_14.

[24] S. B. Obakiro *et al.*, “Deciphering the the molecular mechanism of aloe-emodin in managing type II diabetes mellitus using network pharmacology, molecular docking, and molecular dynamics simulation approaches,” *In Silico Pharmacology*, vol. 13, no. 1, Mar. 2025, doi: https://doi.org/10.1007/s40203-025-00337-1.

[25] T. Huang *et al.*, "MOST: most-similar ligand based approach to target prediction," *BMC Bioinformatics*, vol. 18, no. 1, Mar. 2017, doi: https://doi.org/10.1186/s12859-017-1586-z.

[26] L. E. Bultum, G. B. Tolossa, G. Kim, O. Kwon, and D. Lee, "In silico activity and ADMET profiling of phytochemicals from ethiopian indigenous aloes using pharmacophore models," *Scientific Reports*, vol. 12, no. 1, Dec. 2022, doi: https://doi.org/10.1038/s41598-022-26446-x.

[27] M. Roney, A. R. Issahaku, U. Govinden, A. M. Gazali, M. F. F. M. Aluwi, and N. B. Zamri, "Diabetic wound healing of aloe vera major phytoconstituents through TGF-β1 suppression *via in-silico* docking, molecular dynamic simulation and pharmacokinetic studies," *Journal of biomolecular structure & dynamics*, vol. 42, no. 24, pp. 13939–13952, 2024, doi: https://doi.org/10.1080/07391102.2023.2279280.

[28] Z. M. Lee, B. H. Goh, and K. Y. Khaw, "Aloe vera and the Proliferative Phase of Cutaneous Wound Healing: Status Quo Report on Active Principles, Mechanisms, and Applications," *Planta Medica*, vol. 91, no. 01/02, pp. 4–18, Nov. 2024, doi: https://doi.org/10.1055/a-2446-2146.

[29] N. Özenver, M. Saeed, L. Ö. Demirezer, and T. Efferth, "Aloe-emodin as drug candidate for cancer therapy," *Oncotarget*, vol. 9, no. 25, pp. 17770–17796, Apr. 2018, doi: https://doi.org/10.18632/oncotarget.24880.

[30] F. Nalimu, J. Oloro, I. Kahwa, and P. E. Ogwang, "Review on the phytochemistry and toxicological profiles of Aloe vera and Aloe ferox," *Future Journal of Pharmaceutical Sciences*, vol. 7, no. 1, Jul. 2021, doi: https://doi.org/10.1186/s43094-021-00296-2.

[31] B. Pradhan, "PHYTOCHEMISTRY, PHARMACOLOGY AND TOXICITY OF Aloe vera : A VERSATILE PLANT WITH EXTENSIVE THERAPEUTIC POTENTIAL," *Plant Archives*, vol. 23, no. 2, Oct. 2023, doi: https://doi.org/10.51470/plantarchives.2023.v23.no2.056.

[32] Q. He *et al.*, "Exploring the mechanism of curcumin in the treatment of colon cancer based on network pharmacology and molecular docking," *Frontiers in Pharmacology*, vol. 14, Feb. 2023, doi: https://doi.org/10.3389/fphar.2023.1102581.

[33] X. Shou *et al.*, "Network Pharmacology and Molecular Docking Analysis on Molecular Mechanism of Qingzi Zhitong Decoction in the Treatment of Ulcerative Colitis," *Frontiers in*

Pharmacology, vol. 13, no. 2022.727608, Feb. 2022, doi: https://doi.org/10.3389/fphar.2022.727608.

[34] R. T. M. el-dien *et al.*, "Network pharmacology, molecular docking study, and in vivo validation of the wound healing activity of the Red Sea soft coral Paralemnalia thyrsoides (Ehrenberg 1834) ethanolic extract and bioactive metabolites," *Beni-Suef University Journal of Basic and Applied Sciences*, vol. 13, no. 1, Jun. 2024, doi: https://doi.org/10.1186/s43088-024-00512-x.

[35] J. Xie, J. Wu, S. Yang, and H. Zhou, "Network Pharmacology-Based Study on the Mechanism of Aloe Vera for Treating Cancer," *Evidence-Based Complementary and Alternative Medicine*, vol. 2021, pp. 1–8, Dec. 2021, doi: https://doi.org/10.1155/2021/6077698.

[36] S. C. Pillai, P. K. K. Namboori, N. C. A. Kumar, K. V. Gopal, A. S. Kumar, and P. Bharath, "Investigating multi target drug action of Aloe vera using computational analysis," *2011 2nd National Conference on Emerging Trends and Applications in Computer Science*, vol. 2011.5751406, no. 2011.5751406, pp. 1–4, Mar. 2011, doi: https://doi.org/10.1109/ncetacs.2011.5751406.

[37] A. M. Ahmed *et al.*, "Attenuation of inflammatory response via *Corchorus olitorius* seeds-derived *Penicillium* sp. metabolites in immunocompromised rats," *Natural Product Research*, vol. 40, no. 6, pp. 1485–1489, Dec. 2024, doi: https://doi.org/10.1080/14786419.2024.2431122.

[38] C. Li, J. Pan, C. Xu, Z. Jin, and X. Chen, "A Preliminary Inquiry Into the Potential Mechanism of Huang-Lian-Jie-Du Decoction in Treating Rheumatoid Arthritis via Network Pharmacology and Molecular Docking," *Frontiers in cell and developmental biology*, vol. 9, Jan. 2022, doi: https://doi.org/10.3389/fcell.2021.740266.

[39] Y. Wu *et al.*, "Network Pharmacology Prediction and Molecular Docking-Based Strategy to Discover the Potential Pharmacological Mechanism of Huai Hua San Against Ulcerative Colitis," *Drug Design Development and Therapy*, vol. Volume 15, pp. 3255–3276, Jul. 2021, doi: https://doi.org/10.2147/dddt.s319786.